DIESEL SPRAY VISUALIZATION AND SHOCKWAVES

Harri Hillamo,* ***Teemu Sarjovaara, Ossi Kaario, Ville Vuorinen, & Martti Larmi***

Internal Combustion Engine Research Group, Department of Energy Technology, Helsinki University of Technology, Puumiehenkuja 5 A, FIN-02150 Espoo, Finland

*Address all correspondence to Harri Hillamo E-mail: harri.hillamo@iki.fi

Original Manuscript Submitted: 8/31/2009; Final Draft Received: 12/16/2009

The paper discusses some fundamental spray properties and new aspects of measuring the spray behavior. The fuel injection measurements were done with marine common rail diesel injection equipment under nonevaporating conditions in a pressurized test rig. The tests were made at room temperature to ensure a constant environment for the sprays and to study the fundamentals of transient fuel jet. Fuel injection was performed with 1400 bar pressure to 35 kg/m^3 ambient gas density with different nozzle orifices. Some fundamental phenomena in dense and high-velocity diesel spray can be confirmed by short exposure spray imaging. Imaging was based on planar illumination and digital imaging. The main findings were high-definition shockwave images. Shockwaves can be seen when the supersonic fuel spray exits the nozzle orifice. Shockwave imaging is used to estimate the velocity difference of the fuel and ambient gas. Boundary layer velocity measurements are shown at the vicinity of the nozzle orifice. Velocity measurements can be used to estimate nozzle discharge coefficients. The initial laminar core flow of the liquid and the collapse of this initial region were recorded. This may seem like a rather unlikely phenomenon in diesel injectors and it can well be considered as a special case. Spray-to-spray variation of the spray exit has also been recorded. Some time scales of the transient spray phenomena are also drawn.

KEY WORDS: *diesel spray, shockwaves, spray visualization, common rail, backlight imaging, shadowgraphy, diesel spray velocity*

1. INTRODUCTION

Diesel sprays have been under active research for decades. Some experimental techniques enable higher resolution on spray imaging. More precisely measured spray characteristics are becoming interesting because of the development of computational fluid dynamics. This study discusses results of backlight imaging of sprays. Some of the general spray properties have been reported and discussed in a different paper (Hillamo et al., 2008).

In this paper the main focus is on a few phenomena which can be seen in sprays. These do not show a direct effect on diesel engine performance and are therefore not often recorded or reported. However, these phenomena are important if the fundamental spray behavior is in focus. Basic knowledge of spray physics is important for detailed spray simulations, too. Digital imaging also has certain advantages, because it can handle a high number of samples, and the pressurized gas is found to give a good platform for fuel jet studies (Shao et al., 2003).

Measurements just after the start of injection are shown. Usually the phenomena at the start of injection (spray development) are neglected because the spray has low penetration, and phenomena at spray introduction are thought to have a minor effect on the main combustion process. It should be recognized that even though the

NOMENCLATURE

a	velocity of sound, m/s	U_{fuel}	velocity of fuel, m/s
a_{measured}	measured velocity of sound, m/s	**Greek Symbols**	
ASOI	time after start of injection, s	α	angle between boundary layer and shockwaves, deg
p_{inj}	injection pressure, bar		
p_{gas}	pressure of gas, bar	ρ_{fuel}	density of fuel, kg/m^3
p_{fuel}	pressure of fuel, bar	ρ_{gas}	density of gas, kg/m^3
T_{gas}	temperature of gas, K	**Dimensionless Numbers**	
$U_{\mathrm{indicated}}$	indicated velocity, m/s	Ma	Mach number, dimensionless velocity Ma = U/a
$U_{\mathrm{fuel,max}}$	theoretical maximum of the jet exit velocity, m/s	C_v	velocity coefficient of specific injector
		γ	rate of specific heats, $\gamma = c_p/c_v$

penetration of spray is initially low, some characteristics for the spray are already formed at that stage, e.g., the spray angle is formed at the very beginning of jet development. For precise fuel spray computational fluid dynamics the boundary conditions are becoming more important.

In the current paper near nozzle effects are measured and discussed. When measuring near nozzle effects, various factors affect the exit of fuel from the nozzle orifices. It is clear that the needle valve and the liquid fuel have certain inertia which must be accelerated to enable full flow of fuel. The needle lift is one restriction for fuel flow, and the pressure inside the nozzle will drop due to instant loss of mass at the beginning of injection. The stabilization of pressures will take some time. These phenomena are difficult to measure and therefore the beginning of injection is not clearly understood. A good tool for flow research inside the nozzle seems to be model tests (Suh and Lee, 2008a) and simulations (Ning et al., 2008).

In the beginning of injection, fuel may have a relatively low Reynolds number, and because of the relatively low length-to-diameter ratio (initially still) fuel can sometimes be seen to exit from the orifice as a laminar liquid column. This transparent liquid then becomes unstable and the following higher velocity fuel is pushing the slow part at the front. This leads to breakdown of the initial region and complete spray atomization is seen to take place. It can be seen that atomized fuel has high velocity since it forms shockwaves to ambient gas. When these shockwaves can be seen to bend it means that the velocity of the discharging liquid has exceeded the speed of sound. The exit velocity is further increased, but the spray atomization and ligament breakup has already started at supersonic velocities.

In general, supersonic sprays cause shockwaves. Generation of shockwaves by diesel sprays, as seen in the current paper, has also been studied by other research groups, as it is described in the following chapters. However, the significance of shockwaves to diesel combustion has remained rather unknown. In this paper high-definition shockwave images are introduced which are recorded directly with visible (laser-based) light and a method to estimate jet exit velocity. In other studies x-ray imaging and Schlieren imaging have also been used for imaging of diesel spray shockwaves (MacPhee et al., 2002).

Generation of diesel spray shockwaves has also been validated at high temperatures (Pickett et al., 2009), and similar cases have also been studied with different injection pressures and gas densities (Kook and Pickett, 2008). Gas density has a major effect on spray characteristics, while it changes spray penetration and makes the spray widen with increasing density. The effect of gas density on spray characteristics can be clearly measured and visualized (Araneo et al., 1999).

In the current paper phenomena at the very beginning of diesel spray are shown. Measurements have been performed using backlight photographing. This paper shows a setup which enables high-contrast spray imaging and conversion of particle image velocimetry setup into a backlight imaging setup. Similar phenomena, like initial spray formation, breakup of the liquid core, and flow field formation has been studied with x-rays at atmospheric pressure (El-Hannouny et al., 2003), while the current paper gives a high-definition view with visible light to the same phenomena. In the study of El-Hannouny et al. the x-rays were used because diesel sprays are optically very dense in the vicinity of the jet exit. High-definition photography of the diesel jet near the nozzle has also been done, but the results show different spray behavior due to a different nozzle configuration, light source, and fuel (Bae and Kang, 2006).

When measuring diesel sprays, the effect of ambient gas density to diesel spray formation should be taken into account. The gas density effects have also been studied, and some similarities were found in this study compared to other studies introduced formerly. The importance and formation of diesel-spray-induced shockwaves has been discussed and demonstrated (Roisman et al., 2007). Gas density was also varied and the effects on spray formation and spray tip velocity were studied. The collapse of initial liquid flow when colliding with dense gas has formerly been sketched and discussed (Roisman et al., 2007), and the experiments shown in this paper support the introduced hypothesis and calculations.

Measurements based on shockwave generation and discussion of spray exit velocity are shown in a latter part of the paper. Spray exit velocity has also been studied with laser flow tagging in the vicinity of the nozzle orifice (Wissel and Grünefeldt, 2006). Velocity profiles and the relative velocity difference of mixed gas and liquid fuel can be achieved with a flow tagging technique, and thereby also the jet velocity can be compared to the theoretical maximum velocity. However, there are very few techniques capable of diesel spray jet exit velocity measurements, and it is shown that the generation of shockwaves gives a new perspective on velocity studies.

Diesel fuel jet exit velocity is important for certain phenomena like atomization of fuel and turbulent combustion. Some parameters which are substantial for proper combustion of fuel have been acknowledged for a long time. These kinds of parameters are initial velocity (momentum source), spreading and penetration of fuel (Heywood, 1988; Hiroyasu and Arai, 1990), and nozzle efficiency (LeFebvre, 1989). Initial flow conditions, diameter-to-length ratio of the nozzle orifice, and jet exit velocity have a significant effect on so-called primary breakup of the spray liquid core (Hiroyasu and Arai, 1990; Faeth et al., 1995). Nozzle flow coefficients have been used to describe these phenomena in general. Secondary breakup of droplets is greatly affected by aerodynamic forces, which depends on initial velocity (momentum) of the spray (Pilch and Erdman, 1987). At present the injection pressures are high from the start of injection, and it is believed that the intact liquid core of the spray is very short and complete atomization of liquid is seen a few nozzle diameters downstream (Smallwood and Gülder, 2000).

2. EXPERIMENTAL SETUP

Measurements with the current setup were performed with a marine common-rail injector. Different injection pressures, injector nozzles, and ambient gas densities were tested. The gas density and injection pressure in the measurements shown in this paper are near to real engine conditions (Table 1).

The spray tests were done in a pressurized measurement test rig (Fig. 1) to imitate similar physical conditions seen in engines but in a nonevaporating environment. The gas density was kept constant with the aid of pressure and temperature measurements. The gas pressure was slightly adjusted if needed with a spring-actuated backpressure valve. Different nozzle orifice sizes were tested.

In the optical measurements illumination of images was done with a planar light source (Fig. 2). There was a short duration laser pulse, and the width of the beam was expanded to about 100 mm. While originally green light (532 nm) was shot to a fluorescent plate, the light was phase shifted to white light. This was done to get even and planar light to measurements. The light was further smoothed with a milk glass diffusor. Without phase shifting laser light will cause significant laser speckling which will ruin image quality and make detailed image consideration difficult. Phase shifting takes place nearly instantly, and it was possible to capture consecutive images with time intervals of 500 ns.

The accurate timing and the sequence of measurements were controlled by a computer which was also used for data acquisition. The original request to measure was sent to a trigger unit which synchronized the injector and timing of the laser and the camera. Images were taken at different times after the start of injection (ASOI) and thereby an additional delay was set to camera and laser. Delay was controlled by a timing unit. A schematic image of signal routes is shown (Fig. 3).

2.1 Imaging

Imaging was performed with a 4 megapixel grayscale camera. Imaging parameters are listed in Table 2. The image is rectangular and the resolution of the camera is 12 bit. In the current study the area of view was about 10 $\times$ 10 cm, which corresponds to a pixel resolution of 50 $\times$ 50 μm. In high-detail studies, i.e., shockwave imaging, the area of view was 30 $\times$ 30 mm, which corresponds to a 15 μm pixel resolution. The double frame camera is capable of taking two consecutive images with a time interval of 200 ns. The light source is a double-pulsed

TABLE 1: Operation conditions in measurements

Gas (N_2) density	35 kg/m^3
Gas temperature	$\sim$ 303 K
Fuel (diesel) density	831 kg/m^3
Injector	Marine common-rail injector
Injection pressure	1400 bar
Nozzle orifice diameter	0.31 ... 0.36 mm (indicated at text)

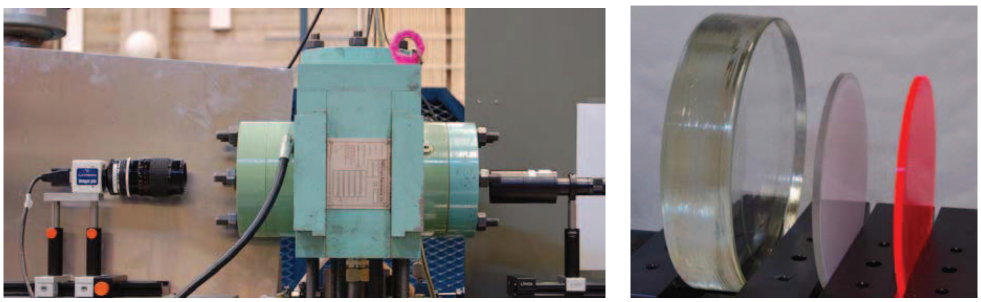

FIG. 1: Measurement chamber was pressurized and the camera, and laser were pointed to each other from different sides of the chamber. Laser light was phase shifted to white light with a fluorescent plate. The light was further smoothed with a milky glass diffusor.

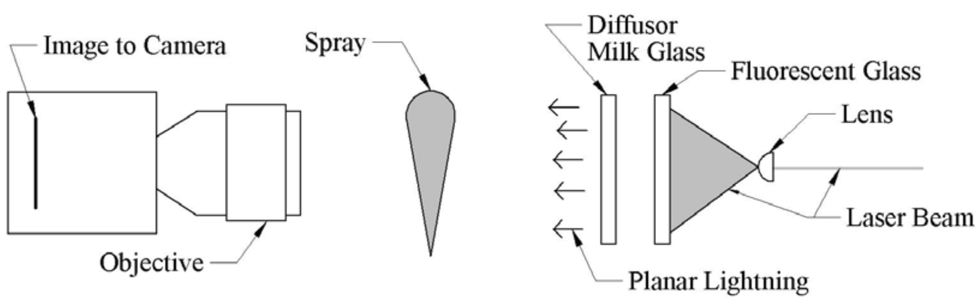

FIG. 2: Schematic image of measurement configuration. View from top.

Nd:yttrium aluminum garnet (YAG) laser which has a maximum pulse energy of 500 mJ (532 nm light). The pulse has a typical duration of 5 ns, which is an advantage because such a short light pulse is capable of freezing most motion of high-velocity fuel spray. Due to the short pulse duration of the light source, high timing accuracy can be achieved.

Very high-definition images were achieved because of short illumination times, high grayscale definition, and special backlighting (Fig. 4). There are many backlighting techniques for imaging high-velocity objects, but this system was used in a rather simple way, where the light source and camera are axial and no special optics have been used. The light source is planar, since it is a flat plate which is illuminated with laser light and the phase shifting nature of the current plate makes the light source planar. The technique is similar to direct shadowgraphy (Settles, 2001). Some other research groups have used laser-based imaging (Suh and Lee, 2008b), spark light (Bae and Kang, 2006), a xenon lamp (Ryu et al., 2005), and radiography (El-Hannouny et al., 2003;Vuorinen et al., 2006).

3. RESULTS

A variety of different image sets was achieved. The sets were divided into different groups according to which physical phenomena was being observed. Measurements

TABLE 2: Imaging parameters

Nd:YAG laser wavelength	532 nm
Duration of laser pulse	5 … 10 ns
Exposure time	Same as laser pulse duration
Camera type	ImagerPro 4M
Imaging technique	Direct imaging (direct shadowgraphy)
Double framing PIV camera	2000 times 2000 pixels
Camera lens	105 mm 1:2.8 Micro-Nikkor lens
Camera aperture	f/2.8

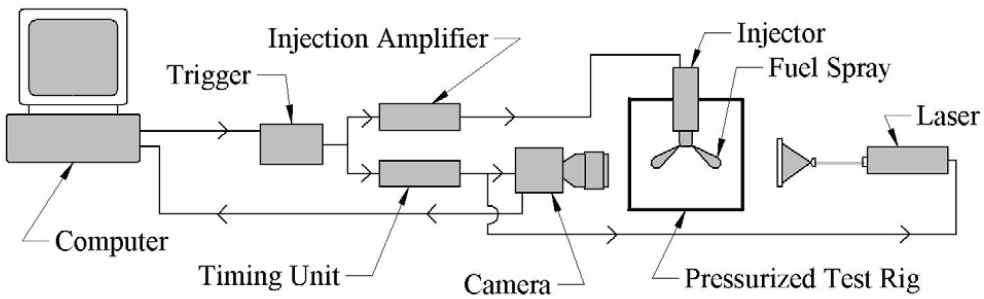

FIG. 3: A schematic image of signal routes and timing of measurements.

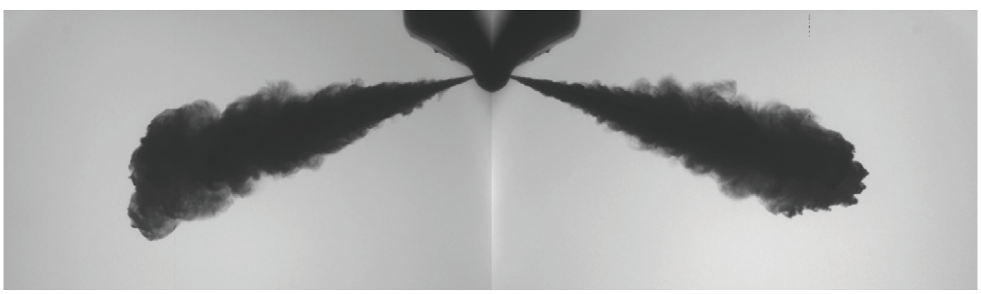

FIG. 4: Two spray images combined and tilted to normal operational position. The measurements were positioned and performed so that only one spray was visible at a time.

were done with a modified nozzle tip. The modification consisted of plugging nozzle orifices next to the spray which was in focus (Fig. 5).

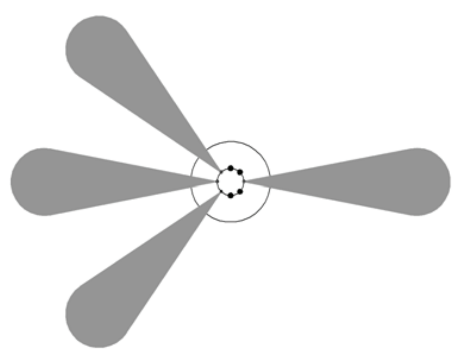

FIG. 5: Spray pattern of a plugged multihole nozzle.

The measurements shown were done as part of a bigger spray measurement project. In the whole project thousands of images were taken. The phenomena seen here and the idea of diesel spray visualization was realized during the project; therefore, more detailed measurements were done to confirm the observed phenomena. The repeatability of these phenomena was high, and the phenomena were seen with different injectors, different fuels, and different nozzles. The authors believe that the phenomena are general, since they are visible with various configurations and have also been sketched, measured, and simulated by other research groups (further references specific to each phenomena are described in the Introduction).

3.1 Start of Injection

At the start of injection a mushroom-cloud-shaped fuel discharge can be seen when the low-velocity liquid tip of the fuel is protruded through the nozzle orifice to ambient gas (Fig. 6). In the measurements there is 1400 bar injection pressure in the common rail and the density of ambient gas is 35 kg/m^3. The images shown are not from the same spray, and the laminar spray exit is a special case, since often the spray introduction is asymmetric, as can be seen from detailed images (Fig. 7). Spray-to-spray variation is typical when using a multiorifice nozzle. The nozzle was partly plugged to enable measurements of a single spray and a schematic of the spray pattern is attached (Fig. 5).

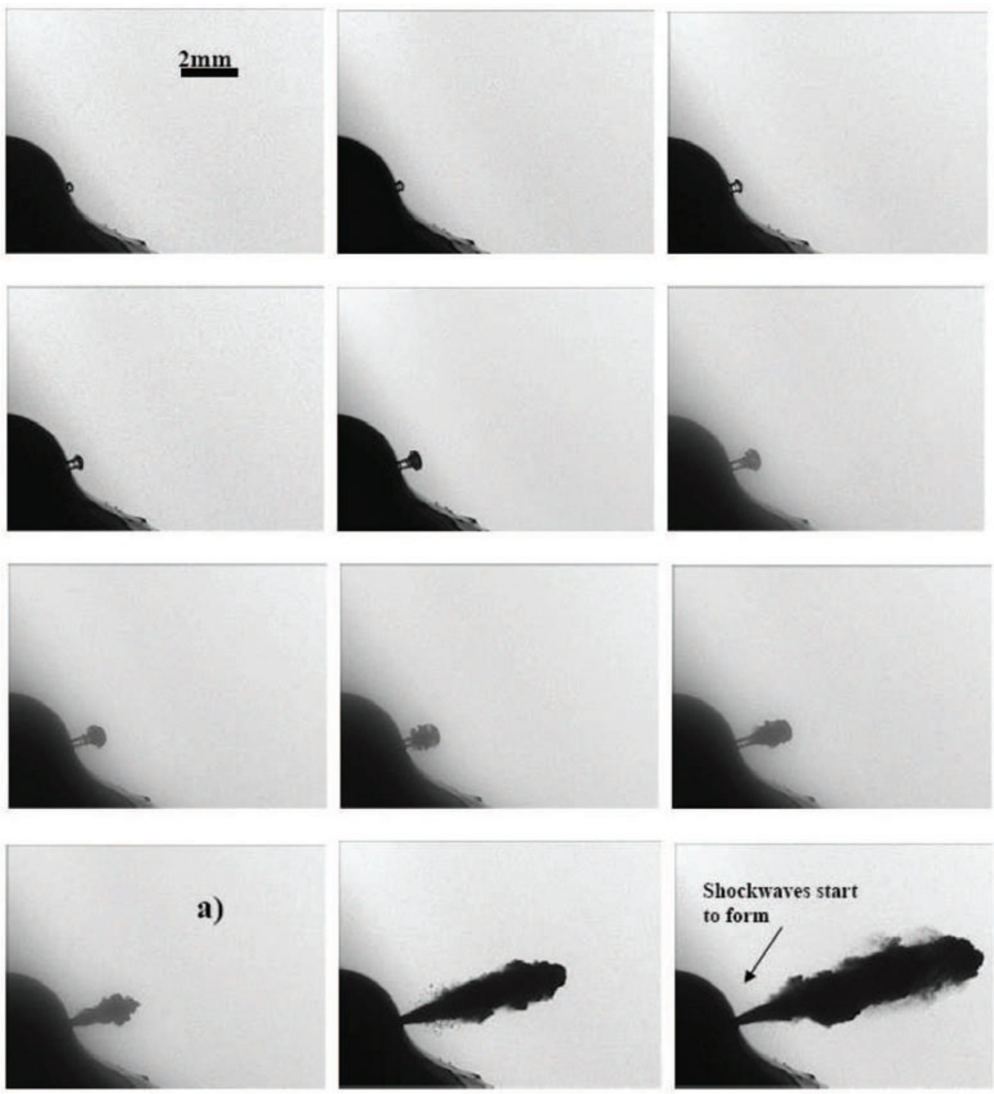

FIG. 6: This particular phenomenon is a special case of spray introduction. Each of these images is from a different spray and the "laminar spray introduction" is found from a large measurement set. Very often the injections looked like the image (a) if initial disturbances had occurred — the laminar exit is a rare but interesting phenomenon and gives new looks to the mass fraction of liquid and gas at the initial stage of spray development.

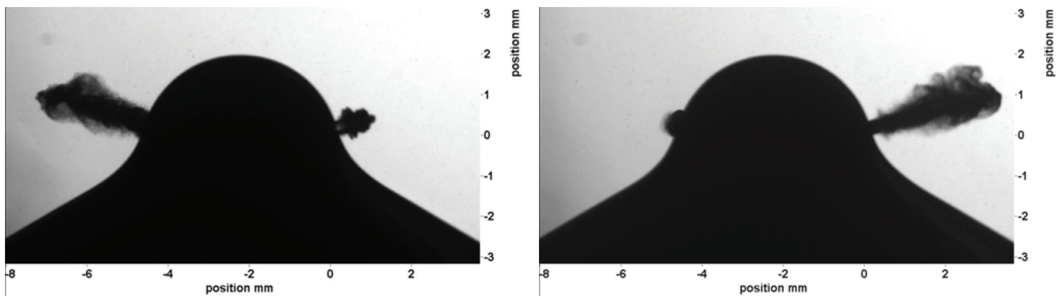

FIG. 7: Example of spray-to-spray variation with equal delay from the start of injection. All the measurement parameters are the same and ideally, the spray images should be similar. Left side of the nozzle tip: three holes open, not parallel to the imaging plane. Right side of the nozzle tip: one nozzle hole open and parallel to the measurement plane.

It is acknowledged that there is some effect on the spray behavior due to plugged orifices. The phenomena described in the current paper do not suffer significantly from this issue, since the results describe sprays as a general phenomena and the focus is more on the measurement technique. Also if we look at Fig. 7, it can be seen that there is an arbitrary effect on spray-to-spray variation. It seems that the plugging has not favored certain nozzle orifices. Plugged nozzles have been successfully used for study of nozzle orifice characterization (Hillamo et al., 2008). According to Fig. 6, supersonic velocities develop shortly after the start of injection, which indicates that the nozzle starts to operate as multiple "plain orifice pressure atomizers". In plain orifice pressure atomizers the main restriction for flow is the nozzle orifice, where also the main pressure drop is seen (LeFebvre, 1989).

In the measured cases the liquid is often first clearly laminar, and later there is some Kelvin–Helmholtz instability introduced (Fig. 6). The liquid core starts to roll up from the tip of the liquid column and the instabilities begin to grow larger. Similar results have also been achieved with large-eddy simulations (Srinivasan et al., 2008), and modeling of dense liquid sprays shows similar phenomena (Tonini et al., 2008). Later the liquid core of the spray is changed to nontransparent. That can be taken as a clear sign of breakup of liquid fuel. Only undisturbed liquid can act as optically transparent media at the current measurement setup. The primary atomization is believed to happen due to cavitation and high-velocity instabilities (mainly turbulence) of the liquid. The liquid part of the fuel does not tolerate the high aerodynamic forces and internal turbulence, since it leaves the nozzle hole and therefore bursts into a spray of droplets and ligaments. It is believed that the liquid core of the spray is disturbed by cavitation and initial breakup, and an intact liquid core can occasionally be seen. Even if some disturbances and breakup had occurred, the liquid-to-gas mass fraction at the vicinity of the injector should be near the same level in the case of low and high atomization. In the images (Fig. 6) the injection pressure is 1400 bar, gas density is 35 kg/m^3, and the nozzle orifice diameter is 0.32 mm.

Even though this laminar liquid column (Fig. 6) is a common feature in early spray development, no general conclusions can be made. Sometimes the spray is atomized at a very early stage and even low atomization or the breakup of a spray core will result in a nontransparent and asymmetric jet exit. If atomization occurs the view through the liquid part is lost and no visual analysis of the inner structures of the spray column can be made with the current measurement system. These laminar and low-atomization cases were not separated or excluded from the subsequent spray analysis, and those seem to have similar behavior to more atomized sprays with regard to spray penetration and geometry (Hillamo et al., 2008). The main acceleration region of spray penetration for these marine diesel injectors was found to be less than 12 mm (100 S/d) from the nozzle (Hillamo et al., 2008), and the transparent core is seen to break down at maximum of roughly 4 mm (35–40 S/d).

At this point it must be clarified that the jet exit velocity and the spray penetration velocity are very different measurements. The jet exit velocity is coupled with mass flow, and the tip velocity is coupled with atomization, momentum of liquid, and aerodynamic effects. The penetration of fuel spray is an important measure for the combustion, since for satisfactory combustion a large spatial coverage of spray is needed.

Some time scales can be drawn from the initial introduction of fuel. The velocimetry measurements (Hillamo et al., 2008) show that the initial liquid column (Fig. 6) has tip velocities which are about 40–50 m/s. The shift from low exit velocity to supersonic flow (shockwaves at Fig. 6) was seen to take place within less than 100 μs. The spray tip velocity is constantly accelerated from velocities of 50 m/s to 150–200 m/s, even though the jet exit velocity can be seen to reach supersonic velocities much earlier than the peak velocity of the spray tip as measured (Hillamo et al., 2008).

3.2 Shockwave Generation and Jet Exit Velocity

Diesel fuel sprays are supersonic because of the high injection pressures. Supersonic fuel jets cause shockwaves to ambient gas, and this can be both measured and computationally confirmed (Im et al., 2009). According to Bernoulli's law (Eq. 1), the maximum of the jet exit velocity ($U_{\rm fuel,max}$) is bound with the pressure difference at the nozzle orifice. According to several studies there are some issues that limit the maximum velocity. The most important of these issues are hydraulic flip and cavitation, which cut down the flow area which then cuts down the jet exit velocity compared with the theoretical maximum (Naber and Siebers, 1996; Martynov et al., 2006; Kastengren et al., 2007).

The Bernoulli equation (Eq. 1):

$$U_{\rm fuel,max} = \sqrt{2 \cdot \frac{(p_{\rm fuel} - p_{\rm gas})}{\rho_{\rm fuel}}} \quad (1)$$

The theoretical maximum velocity of jet in the current measurements can be calculated from Eq. 1:

$$\begin{aligned} U_{\rm fuel} &= C_v \cdot \sqrt{2 \cdot \frac{(p_{\rm fuel} - p_{\rm gas})}{\rho_{\rm fuel}}} \\ &= \sqrt{2 \cdot \frac{(1400E^5 - 31.4E^5)}{831}} = 574\frac{m}{s} \end{aligned}$$

where C_v is a characteristic nozzle velocity coefficient which can be approximated. To estimate theoretical maximum velocity, C_v is set to unity. The pressure difference at the nozzle is indicated with $p_{\rm fuel} - p_{\rm gas}$ [Pa], and fuel density is indicated with $\rho_{\rm fuel}$ [kg/m^3] (Naber and Siebers, 1996).

The jet exit velocity of the fuel spray can also be estimated from the bending of shockwaves. The shockwaves (Fig. 8) will set to a certain angle (Eq. 2) depending on the Mach number of the boundary layer (Liepmann and Roshko, 1960). The novel idea is that with shockwave imaging measurements it is possible to get velocity data from the vicinity of the jet exit. Some shockwaves can be recognized as near as one nozzle hole diameter downstream (Fig. 10). While the nozzle orifices at diesel injectors are in the range of 0.1–0.4 mm in diameter, there are few measurement techniques capable of velocity estimates so near the jet exit (Kastengren et al., 2007). Despite that, near-nozzle velocity measurements of diesel injectors have been demonstrated (Meingast et al., 2000; Wissel and Grünefeld, 2006).

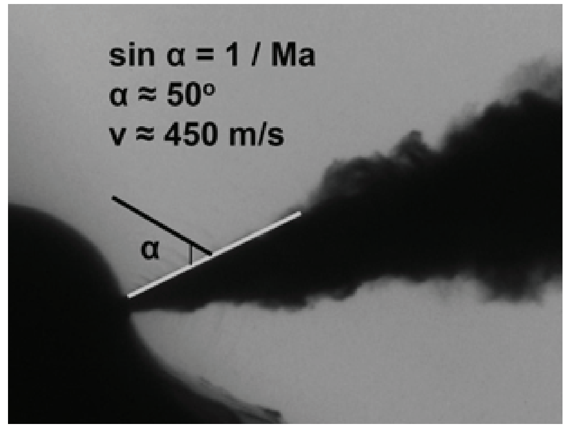

FIG. 8: Schematic of jet velocity estimation.

The edge of the spray represents the boundary layer which is progressing at a high velocity, and the surrounding gas is initially stationary. Since the fuel spray is supersonic and the shockwaves travel at a local speed of sound, the waves are lagging behind (seen as bending). Shockwaves will catch the spray tip while it has decelerated further downstream. Correlation between velocity and shockwave angle is

$$\sin\alpha = \frac{1}{\rm Ma} \quad (2)$$

where α is the angle between boundary layer and shockwave (Fig. 8), and Ma is the dimensionless number indicating the boundary layer velocity compared to local speed of sound (Liepmann, Roshko, 1960).

Here it is estimated that the speed of sound is a = 355 m/s, while $\rho_{\rm gas}$ = 35 kg/m^3 and $T_{\rm gas}$ = 30°C in the ambient nitrogen environment. The 50° bending of shockwaves corresponds to a velocity of 450 m/s. The definition of angle is not very accurate, but it is clear that the right value lies between 40 and 60°. Thereby the jet exit velocity can be estimated to be between 400 and

500 m/s. The injected mass per injection compared to the nozzle orifice size suggests that these estimates have the right order of magnitude.

3.3 Speed of Sound in Pressurized Media

Speed of sound, a, in pressurized (ideal) gaseous media can be estimated with the following equation (Eq. 3):

$$a = \left(\frac{\gamma \cdot p_{\text{gas}}}{\rho_{\text{gas}}}\right)^{0.5} \tag{3}$$

where γ is the ratio of specific heats, p_{gas} is the pressure of gas, and ρ_{gas} is density (White, 2006).

The shockwaves were recorded to move at approximately a_{measured} = 360±20 m/s, while the computational value for the corresponding environment was a = 355 m/s (nitrogen, 35 kg/m^3, 303 K). The edge of a shockwave was very sharp and it was possible to recognize the edge within pixel resolution. Error due to the measurement system is therefore set to ±1 pixel, which corresponds to ±20 m/s. The shockwave propagation has a certain error due to the pixel size of the images and the fact that the images are a kind of projection of the tangent of a spherical or conical wave. From the images a shockwave shift of 0.18 mm was recorded between two images captured with a 500 ns time interval.

Because of the crossing shockwaves the particular waves had a "fingerprint" which enabled recognition of the same shockwave in consecutive pictures (Fig. 9). With the current measurement system it was possible to freeze the shockwaves near to each other if consecutive images were taken with a time interval of, e.g., 500 ns. Then it was possible to iteratively find different time and shockwave shift correlations and to approximate the speed of sound with an optimal wave shift.

3.4 High-Definition Imaging of Diesel-Spray-Generated Shockwaves

If we take a close look at the nozzle, some shockwaves near the nozzle orifice show a relative angle of 44° measured from the boundary layer of the fuel spray (Fig. 10) while in the latter part the waves seem to set more likely to around a 50° angle. These angles correspond to 450–510 m/s (Ma ≈ 1.25–1.45) velocities. The magnitude of velocity a few nozzle orifice diameters downstream is as expected. This is slightly less than the theoretical maximum velocity at the nozzle exit, as it should be. This approximation of velocity is made for the boundary layer velocity. The boundary layer is decelerated because of friction and it has a slightly lower velocity than the core of the fuel jet. It is also known that theoretical maximum velocity is not usually achieved. Nozzle efficiency can be approximated according to comparison between theoretical and measured values.

The measured velocity $U_{\text{indicated}}$ can be compared to the theoretical maximum velocity $U_{\text{fuel,max}}$ and a relation for the velocity coefficient can be calculated (Eq. 4). According to measurements the characteristic velocity coefficient C_v for a specific nozzle (Fig. 10) can be estimated (Naber and Siebers, 1996):

$$C_v = \frac{U_{\text{indicated}}}{U_{\text{fuel,max}}} = \frac{510\text{m/s}}{574\text{m/s}} = 0.89 \tag{4}$$

This result for the velocity coefficient (C_v) may be a bit underestimated because the measured velocity is about two nozzle orifice diameters downstream of the jet exit and because the ambient gas might not be completely still. There might also be additional losses due to flow conditions inside the orifice and primary atomization just after the jet exit.

3.5 Liquid Core of Spray

In part of the measurements transparent liquid can be seen to exit the nozzle. Transparency of liquid in this case means undisturbed liquid flow. Even small amounts of bubbles or initial atomization would form a nontransparent core. The liquid core of the spray will act as a kind of lens which is collecting the light to the center part of the spray, diffusing the light at the edges (compare to Fig. 11). The disintegration of the liquid core is believed to take place at the vicinity of the jet exit, at a maximum of a few nozzle orifice diameters downstream (Smallwood and Gülder, 2000). The disintegration of the intact core was monitored, e.g., with microscopic imaging of the spray exit (Bae and Kang, 2006) and radiography (El-Hannouny et al., 2003;Vuorinen et al., 2006), and there have been some trials of ballistic imaging as well (Linne et al., 2006).

The spray core was often nontransparent in the measurements, and it seemed to be dependent on the nozzle if this liquid core was more often visible. Tested nozzles (a total of five nozzles) had different diameter-to-length ratios and different machining. This probably contributed to flow conditions, i.e., cavitation, inside the hole.

The shockwaves indicate that the outer edges of the spray have a velocity of over 360 m/s, and even though there was cavitation or similar phenomena inside the nozzle, the liquid core is occasionally conserved intact

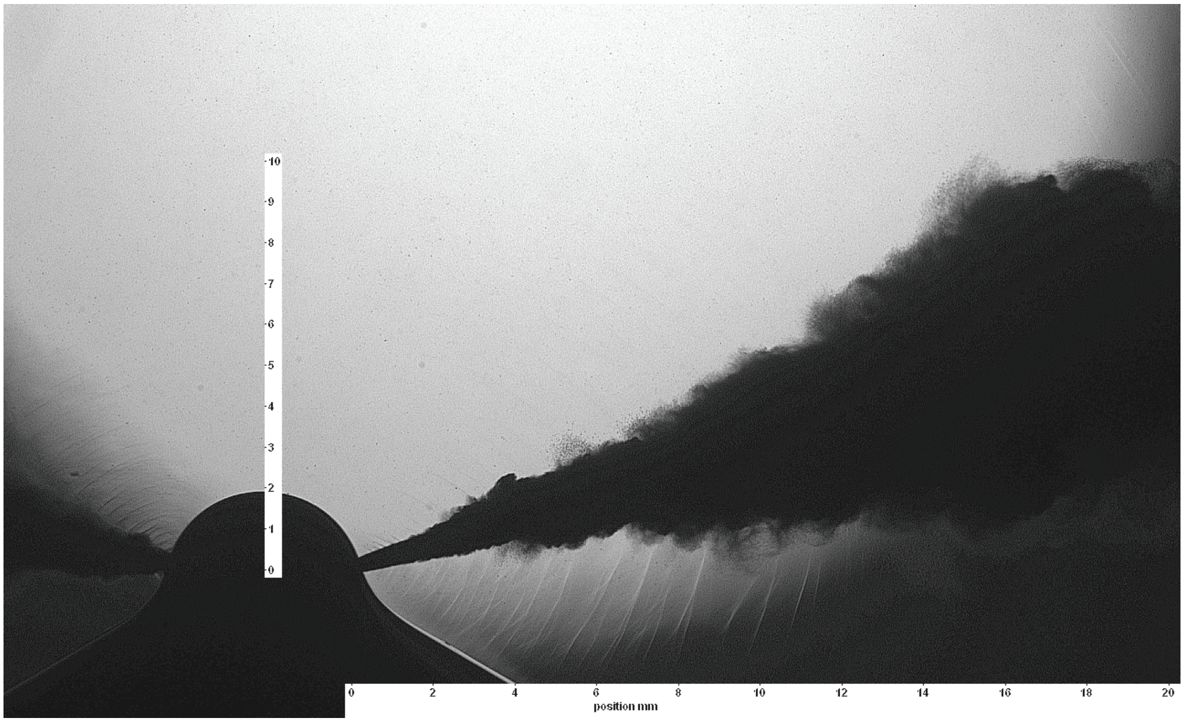

FIG. 9: On the left side a mixing of shockwaves can be seen. On the right side only one nozzle hole is open. Special fingerprint of shockwaves can be seen.

(Fig. 11). Even a few bubbles of ligaments would scatter the light, and it would not be possible to see light through the spray core. The jet exit diameter is the same as the orifice diameter, which means 0.31 mm for scaling purposes. Intact liquid droplets of the same diameter as the spray exit are shown for comparison. The droplets are recorded with the same imaging configuration.

4. CONCLUSIONS

Very good image quality can be achieved with a laser-based backlight imaging system. Results of this paper concentrated on certain phenomena, even though large series of images were gathered during nozzle testing. Due to the larger project with similar measurements at the background, repeatability of the introduced phenomena was known to be good. The flow studies presented here are an interesting summary of some specific fuel spray phenomena.

The laminar jet exit is an occasional phenomenon which is not always present. The jet exit seems to depend on nozzle and injection parameters. Notable spray-to-spray variation is seen in big marine diesel injectors. The jet exit time also has a typically high level of spray-to-spray variation. However, the laminar jet exit and the visualization of the intact liquid core of spray gives a good tool to estimate the mass fraction of liquid and gas at certain distances from the nozzle exit. This can be done since spray angle and penetration can be combined with gas density.

Shockwave imaging of the spray shows potential for spray exit velocity studies and defining the injector delay. It is often assumed that needle lift restrains spray development. When the flow has reached supersonic speed (400–500 m/s) near the theoretical maximum velocity, the flow is probably not significantly restrained by the needle. Because of the nature of a diesel injector as a pressure and orifice atomizer, an adequate pressure difference can be quickly achieved, with careful design. The flow area around the needle should be relatively high compared to the orifice area. These results show that the jet exit velocity is stabilized very early, even though fuel spray penetration was low at the beginning of the jet introduction.

Near-nozzle velocity measurements enable estimations of the velocity coefficient (C_v), which is important when considering nozzle efficiency. Jet exit velocity (initial momentum) is also important when discussing the generation of turbulence in fuel jets.

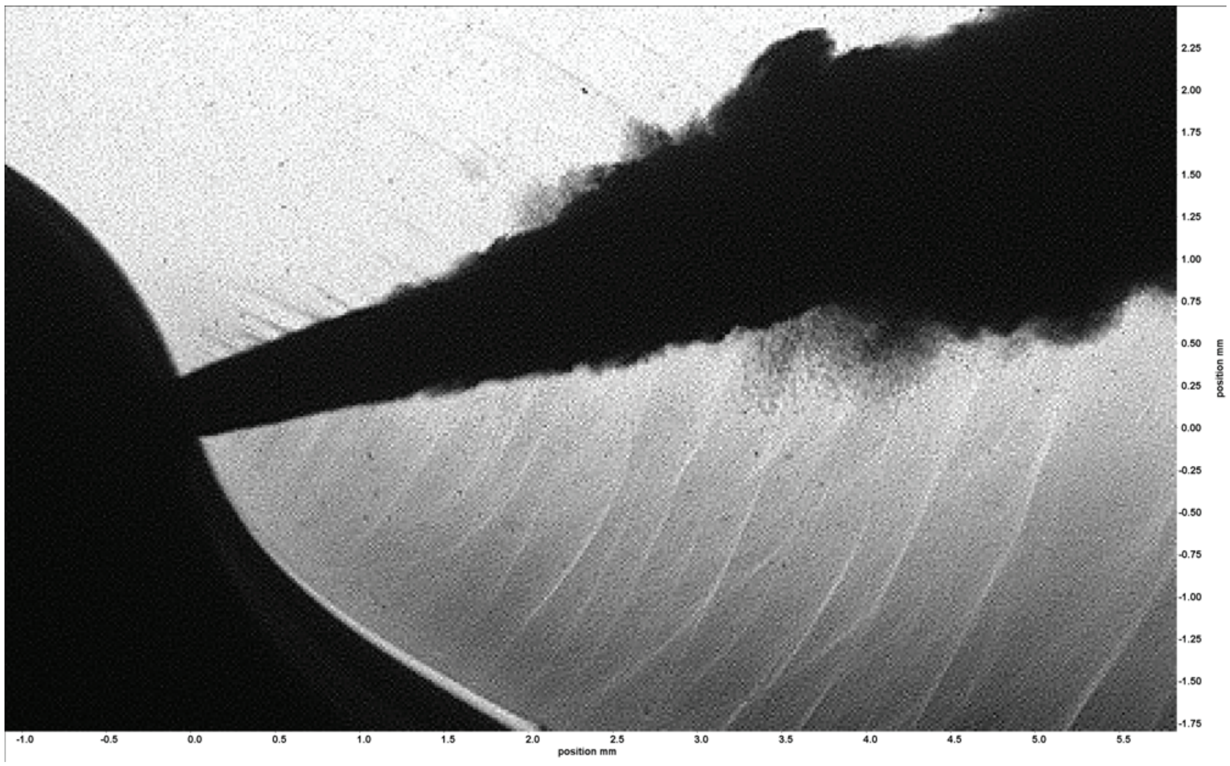

FIG. 10: Close look at the nozzle exit. Hole diameter 0.36 mm. Shockwaves have a maximum angle of 44°.

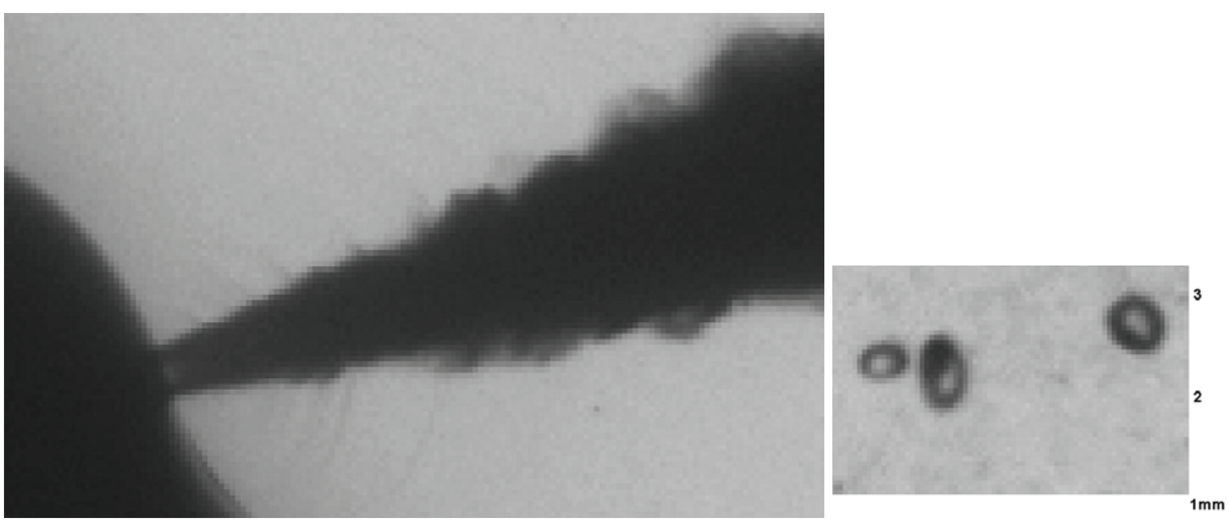

FIG. 11: Liquid (transparent) fuel seen at the jet exit region concurrently with shockwaves. It can be seen that the light intensity pattern of the intact liquid droplets is very similar to what is seen at the jet exit. Nozzle orifice diameter 0.31 mm.

REFERENCES

Araneo, L., Coghe, A., Brunello, G., and Cossali, G. E., Experimental investigation of gas density effects on diesel spray penetration and entrainment, SAE Technical Paper Series 1999-01-0525, p. 15, 1999.

Bae, C. and Kang, J., The structure of a break-up zone in the transient diesel spray of a valve-covered orifice nozzle, *Int. J. Engine Res.*, vol. 7, pp. 319–334, DOI: 10.1243/14680874JER04805, 2006.

El-Hannouny, E. M., Gupta, S., Powell, C. F., Cheong, S.-K., Liu, J., Wang, J., and Sekar, R. R., Near-nozzle spray characteristics of heavy-duty diesel injectors, SAE Technical Paper Series 2003-01-3150, 2003.

Faeth, G. M., Hsiang, L.-P., and Wu, P.-K., Structures and breakup properties of sprays, *Int. J. Multiphase Flow*, vol. 21, 0301-9322(95)00059-3, pp. 99–127, 1995.

Heywood, J. B., *Internal Combustion Engine Fundamentals*, Int. ed., Singapore: McGraw-Hill Series in Mechanical Engineering, p. 930, ISBN 0-07-100499-8, 1988.

Hillamo, H. J., Sarjovaara, T., Vuorinen, V., Larmi, M., Isaksson, S., and Wik, C., Diesel spray penetration and velocity measurements, SAE Technical Paper Series 2008-01-2478m 2008.

Hiroyasu, H. and Arai, M., Structures of fuel sprays in diesel engines, SAE Technical Paper Series 900475, *International Congress and Exposition*, Detroit, MI, p. 11, ISSN 0148-7191, 1990.

Im, K.-S., Cheong, S.-K., Liu, X., Wang, J., Lai, M.-C., Tate, M. W., Ercan, A., Renzi, M. J., Schuette, D. R., and Gruner, S. M., Interaction between supersonic disintegrating liquid jets and their shockwaves, *Phys. Rev. Lett.*, vol. 102, 074501, p. 4, DOI: 10.1103/PhysRevLett.102.074501, 2009.

Kastengren, A. L., Powell, C. F., Cheong, S.-K., Wang, Y., Im, K.-S., Liu, X., and Wang, J., Determination of diesel spray axial velocity using x-ray radiography, SAE Technical Paper Series 2007-01-0666, 2007.

Kook, S. and Pickett, L. M., Effect of ambient temperature and density on diesel-spray-generated shock waves, ILASS Americas, *Annual Conf. on Liquid Atomization and Sprays*, 2008.

LeFebvre, A. H., *Atomization and Sprays*, U.S.A.: Taylor & Francis, ISBN 0-89116-603-3, ISSN 1040-2756, 1989.

Liepmann, H. W., and Roshko, A., *Elements of Gas Dynamics, 1957 Galcit Aeronautical Series, California Institute of Technology*, New York: John Wiley and Sons, Inc., 3rd. ed, 1960.

Linne, M., Paciaroni, M., Hall, T., and Parker, T., Ballistic imaging of the near field in a diesel spray, *Exp. Fluids,* vol. 40, pp. 836–846, DOI: 10.1007/s00348-006-0122-0, 2006.

MacPhee, A. G., Tate, M. W., Powell, C. F., Yue, Y., Renzi, M. J., Ercan, A., Narayanan, S., Fontes, E., Walther, J., Schaller, J., Gruner, S. M., and Wang, J., X-ray imaging of shockwaves generated by high-pressure fuel sprays, *Science*, vol. 295, p. 1261, DOI: 10.1126/science.1068149, 2002.

Martynov, S. B., Mason, D. J., and Heikal, M. R., Numerical simulation of cavitation flows based on their hydrodynamic similarity, *Int. J. Engine Res.*, vol. 7, pp. 283–296, DOI: 10.1243/14680874JER04105, 2006.

Meingast, U., Reichelt, L., Renz, U., and Müller, D., Nozzle exit velocity measurements at a multi-orifice cr-nozzle, *ILASS-Europe 2000,* Darmstadt, 2000.

Naber, J. D. and Siebers, L. D., Effects of gas density and vaporization on penetration and dispersion of diesel fuel, SAE Technical Paper Series 960034, pp. 82–111, 1996.

Ning, W., Reitz, R. D., Diwakar, R., and Lippert, A. M., A numerical investigation of nozzle geometry and injection condition effects on diesel fuel injector flow physics, SAE Technical Paper Series 2008-01-0936, p. 25, 2008.

Pickett, L. M., Kook, S., and Williams, T., Visualization of diesel spray penetration, cool-flame, ignition, high-temperature combustion, and soot formation using high-speed imaging, SAE Technical Paper Series 2009-01-0658, 2009.

Pilch, M. and Erdman, C. A., Use of breakup time data and velocity history data to predict the maximum size of stable fragments for acceleration –Induced breakup of a liquid drop, *Int. J. Multiphase Flow*, vol. 13, no. 6, pp. 741–757, 1987.

Roisman, I. V., Araneo, L., and Tropea, C., Effect of ambient pressure on penetration of a diesel spray, *Int. J. Multiphase Flow*, vol. 33, pp. 904–920, DOI: 10.1016/j.ijmultiphaseflow.2007.01.004, 2007.

Ryu, J., Kim, H., and Lee, K., A study on the spray structure and evaporation characteristic of common-rail type high-pressure injectors in homogenous charge compression ignition engine, *Fuel*, vol. 84, pp. 2341–2350, DOI: 10.1016/j.fuel.2005.03.032, 2005.

Settles, G. S., *Schlieren and Shadowgraph Techniques – Visualizing Phenomena in Transparent Media*, Berlin-Heidelberg: Springer-Verlag, Corrected 2nd ed. printed in Germany, 2006, ISBN 3-540-66155-7, 2001.

Shao, J., Yan, Y., Greeves, G., and Smith, S., Quantitative characterization of diesel sprays using digital imaging techniques, *Meas. Sci. Technol.*, vol. 14, pp. 1110–1116, 2003.

Smallwood, G. J. and Gülder, Ö. L., Views on the structure of transient diesel sprays, *Atomization Sprays*, vol. 10, pp. 355–386, 2000.

Srinivasan, V., Salazar, A. J., and Saito, K., Numerical investigation on the disintegration of round turbulent jets using LOS/VOF technique, *Atomization Sprays*, vol. 18, pp. 571–617, 2008.

Suh, H. K. and Lee, C. S., Effect of cavitation in nozzle orifices on the diesel fuel atomization characteristics, *Int. J. Heat Fluid Flow*, vol. 29, pp. 1001–1009, DOI: 10.1016/j.ijheatfluidflow.2008.03.014, 2008a.

Suh, H. K. and Lee, C. S., Experimental and analytical study on the spray characteristics of dimethyl ether (DME) and diesel fuels within a common-rail system in a diesel engine, *Fuel*, vol. 87, pp. 925–932, DOI:10.1016/j.fuel.2007.05.051, 2008b.

Tonini, S., Gavaises, M., and Theodorakakos, A., Modelling of high-pressure dense diesel sprays with adaptive local grid refinement, *Int. J. Heat Fluid Flow*, vol. 29, pp. 427–448, DOI: 10.1016/j.ijheatfluidflow.2007.11.009, 2008.

Vuorinen, V., Larmi, M., Antila, E., Kaario, O., El-Hannoy, E., and Gupta, S., Near nozzle diesel spray modeling and x-ray measurements, SAE Technical Paper Series 2006-01-1390, p. 12, 2006.

White, F. M., *Viscous Fluid Flow*, Singapore: McGraw-Hill Companies, 3rd Int. ed., p. 629, ISBN 007-124493-X, 2006.

Wissel, S. and Grünefeld, G., Flow-field measurements of liquid and gaseous phases in the ultra-dense region of diesel sprays, *Appl. Phys. B*, vol. 83, pp. 181–184, DOI: 10.1007/s00340-006-2185-2, 2006.